



SIGNIFICANT WAVE HEIGHT RETRIEVAL USING SENTINEL-1 SAR IMAGERY:

Semi-empirical Investigation on Open Ocean Radar-look Directional Wave

Fabian S. Pramudya, Jiayi Pan, Adam T. Devlin
The Chinese University of Hong Kong



香港中文大學
The Chinese University of Hong Kong



Research Objective

1. Evaluating semi-empirical update of significant wave height (H_s) estimation applied to Sentinel-1 SAR repository for narrow-band swell-wave spectrum on the open-ocean waters **without prior knowledge or external inputs.**
2. Evaluate the dependency between H_s and local environment (wind forcing, wave type, SAR system limitation, and imaging mechanism)



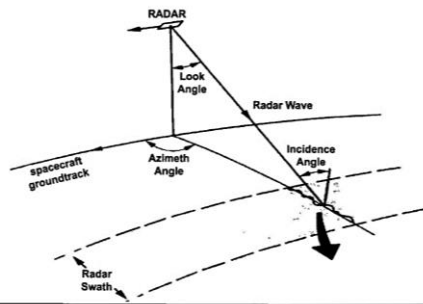
New Approach of a Complimentary Work:

1. Updating the surface roughness and slope variation parameters derived from vertical polarization in a 5.405 GHz SAR system
2. Applying necessary digital filtering method for better peak of dominant wavelength identification in the frequency domain of 2D-Fast Fourier Transform
3. Evaluating the limitation and effects of varying wind speed and dominant wave type related to the nature of inear algorithm



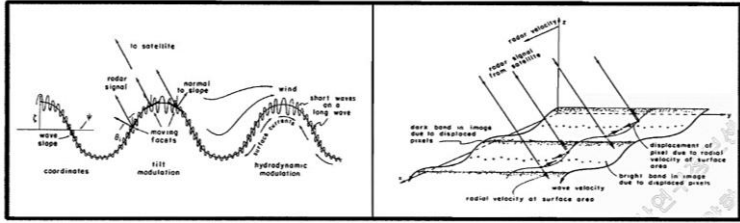
SAR Capturing the Wave

1

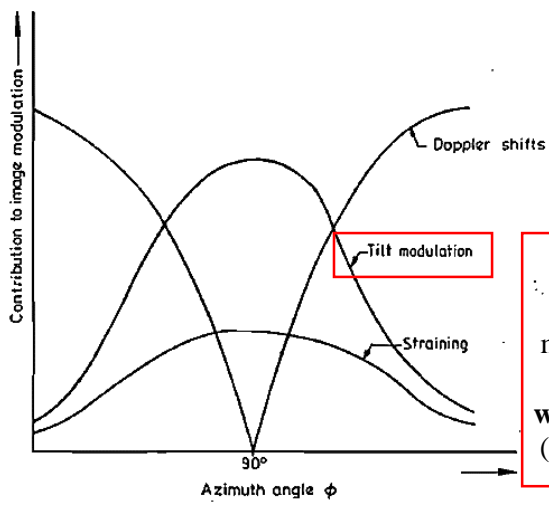
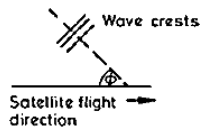


Radar system imaging ocean surface terminology (*upper left*), and Backscattered signal from moving ocean surface (*lower*). Dominated by Bragg scattering from capillary waves and short gravity waves, the composed waves in turn are modulated in their orientation, energy, and motion **by longer waves** on the bottom two images (Kim and Moon, 2003).

In the case of **swell**, the waves has strong space-time correlation and result in constructive velocity bunching. In **wind dominant sea**, however, the velocities are more random. The SAR processing usually becomes more destructive and apparent blurring (Swift and Wilson, 1979., Ardhuin, et al. 2015., Stopa, et al. 2015.)

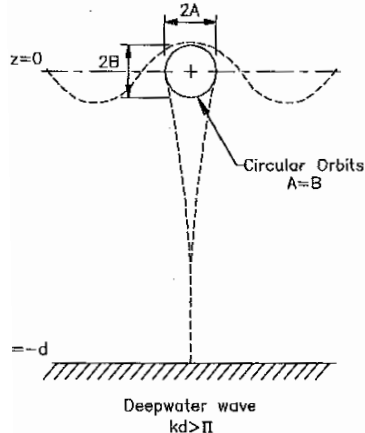


2

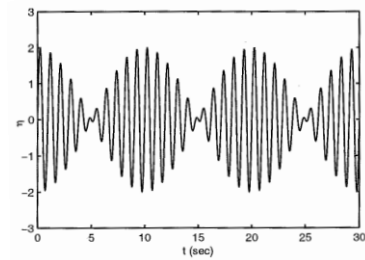


Dominant imaging mechanism on **radar-look wave direction** (Alpers, 1981)

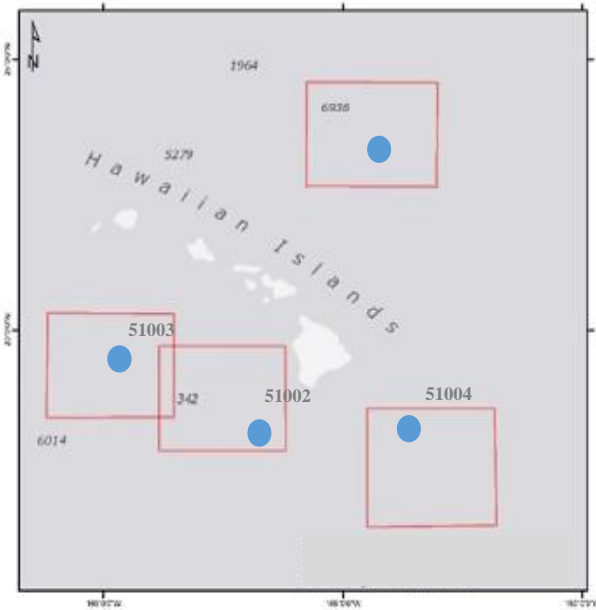
3



Diagrammatic representation of the motion of fluid particle beneath a wave as predicted by **linear wave theory** (Young, 1999 after CERC, 1984) (*upper*) and the formation of wave groups as a result of the superposition of two linear wave trains with different frequencies (Young, 1999 after Kinsman 1965) (*bottom*)



Area and Data

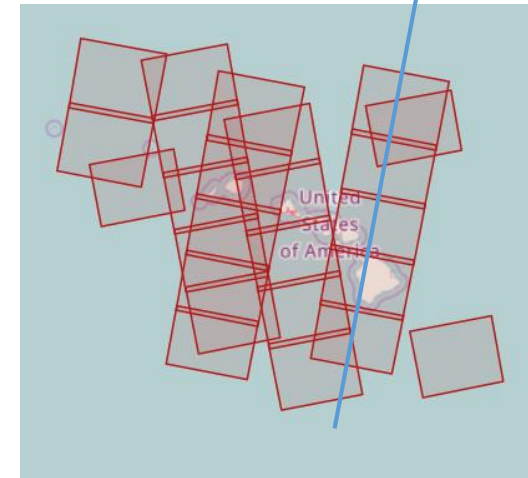


Area of Interest :
Hawaii Waters
(Oct 2016 – December 2017)

Offshore NDBC Buoys
NDBC 51000, 51002,
51004

Available Data : 143 scenes
(69 scenes selected for
radar-look directional wave)

Data Used are Ascending
Sentinel 1A & 1B



Data Example on NDBC Station 51004, HI

NDBC STATION 51004	DATE	TIME	#YY	MM	DD	hh	mm	WDIR	WSPD	GST	WVHT	DPD	APD	MWD	PRES	ATMP	WTMP	DEWP	VIS	TIDE
								#yr	mo	dy	hr	mn	degT	m/s	m/s	m	sec	sec	deg	hPa
S1A_IW_GRDH_1SDV_20161010T	10/10/2016	4:21:50	2016	10	10	3	50	42	7	8.1	2.01	14.8	6.62	351	1011.9	26.6	27	999	99	99
			2016	10	10	4	50	45	7.8	9.1	1.93	14.8	6.57	333	1012.4	26.7	27	999	99	99
S1A_IW_GRDH_1SDV_20161022T	22/10/2016	4:21:50	2016	10	22	3	50	53	10.9	13.2	2.83	12.1	6.5	341	1012.7	27	26.8	999	99	99
			2016	10	22	4	50	54	10.9	13.1	2.89	8.33	6.47	90	1013	26.9	26.8	999	99	99

Contents are taken from: <http://ndbc.noaa.gov/>

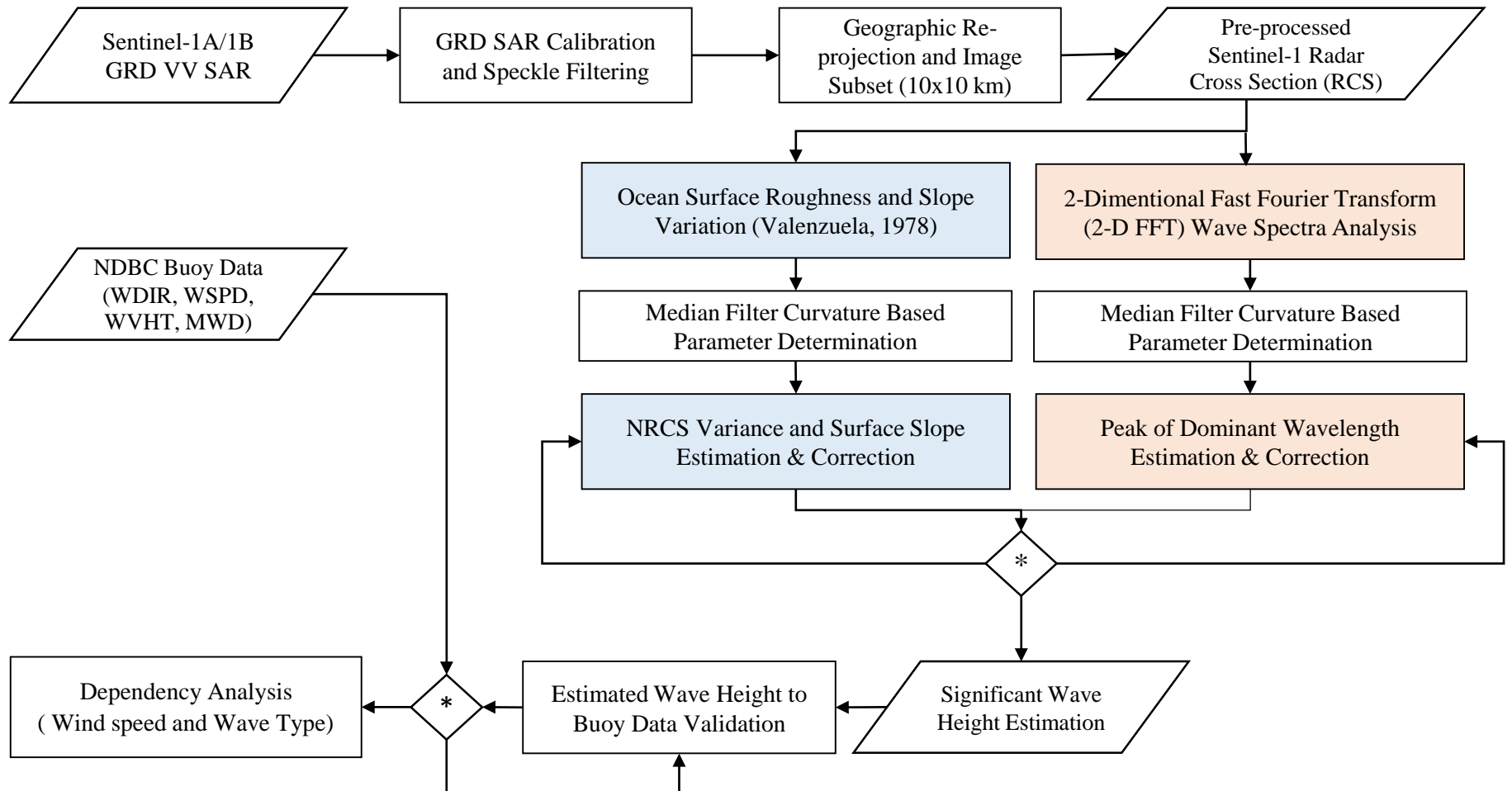


National Oceanic and Atmospheric Administration's
National Data Buoy Center
Center of Excellence in Marine Technology



香港中文大學
The Chinese University of Hong Kong

Flowchart



(*) Statistical assessment (outlier removal/ filtering/ linear regression)
Accuracy accepted or not



Algorithm & Method

For a narrow-band swell-wave spectrum centered on wave number K_0 , the r.m.s slope of the sea surface, $\tan \Theta_r$, is given (Thomas, 1982)

$$\frac{\tan \Theta_r}{H_s} = \frac{|K_0|}{4} = \frac{\pi}{2\lambda_0}$$

Using the equation above, if we know $\tan \Theta_r$ and λ_0 , it is **straight forward to determine λ_0 by taking the 2 dimensional Fast Fourier Transform (2D-FFT) from a digital image**. On the other hand, the determination of $\tan \Theta_r$ is based on the variation of the backscattering cross-section of the sea surface with incident angle (Valenzuela, 1978). Where Θ is angle of the sea surface slope, and very small relative to the wavelength, we could rewrite those equation as follows:

$$\frac{\sqrt{\langle \theta^2 \rangle}}{H_s} = \frac{\pi}{2\lambda_0}$$

Below are several points need to be noted, to obtain the r.m.s. slope of the sea surface

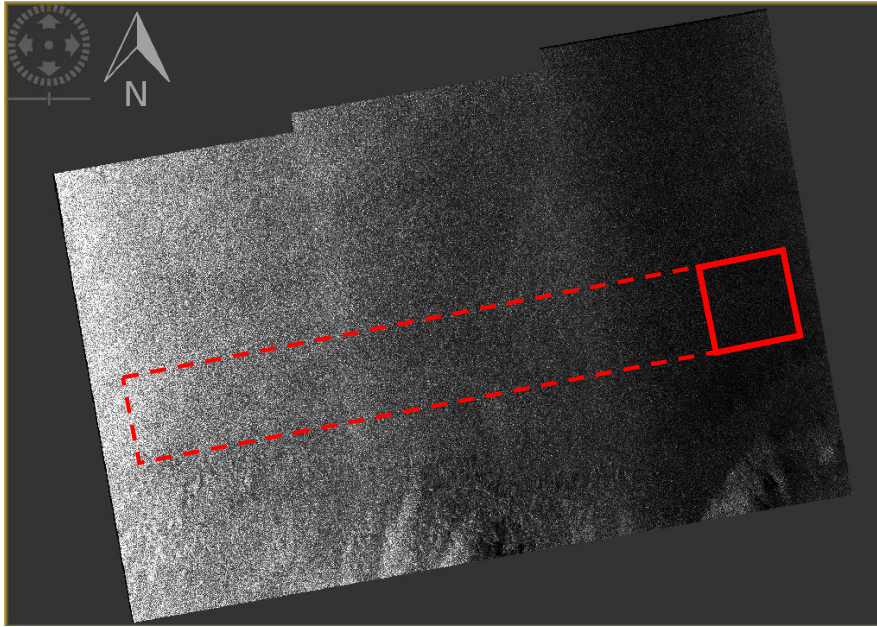
1. Normalized Radar cross-section of sea surface changes with incidence angle [$\sigma_0 = \sigma_0(\Theta)$]
2. where Θ represents the SAR wave incidence angle, the NRCS (σ_0) will change within the various Θ
3. Because of the tilt modulation, there is a small incidence angle change due to the sea surface slope relative to the mean surface. This, if the sea surface slope angle is θ , the incidence angle for the tilted sea surface is [$\Theta = \Theta_0 - \theta$]

$$\sqrt{\langle \theta^2 \rangle} = \sqrt{\langle [\sigma_0(\Theta_0 - \theta) - \sigma_0(\Theta_0)]^2 \rangle} / \left. \frac{d\sigma_0}{d\Theta} \right|_{\Theta=\Theta_0}$$

where $\sqrt{\langle [\sigma_0(\Theta_0 - \theta) - \sigma_0(\Theta_0)]^2 \rangle}$ is the standard deviation of σ_0 , denoted as $\text{std}(\sigma_0)$. Therefore, we have equation below explaining the r.m.s slope of the sea surface as seen in the original equation

$$\sqrt{\langle \theta^2 \rangle} = \text{std}(\sigma_0) / \left. \frac{d\sigma_0}{d\Theta} \right|_{\Theta=\Theta_0}$$

These parameters gives us the simple empirical-physical properties of swell-waves happens, assuming that the wavelength are constant and linearly distributed over a subset of image. Thus, this equation is not suitable for understanding phenomena such as internal waves and very low to extreme sea state condition. Those boundaries of application will be explained later.

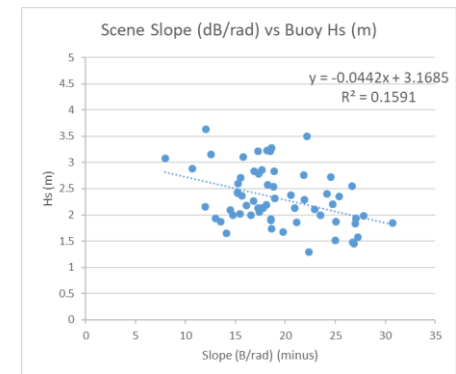
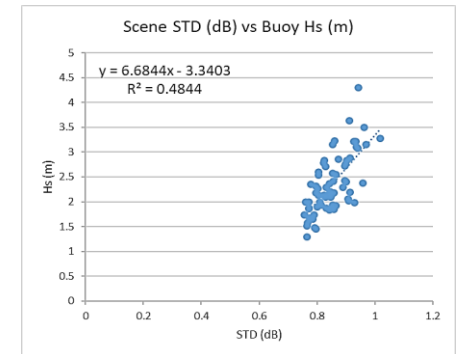
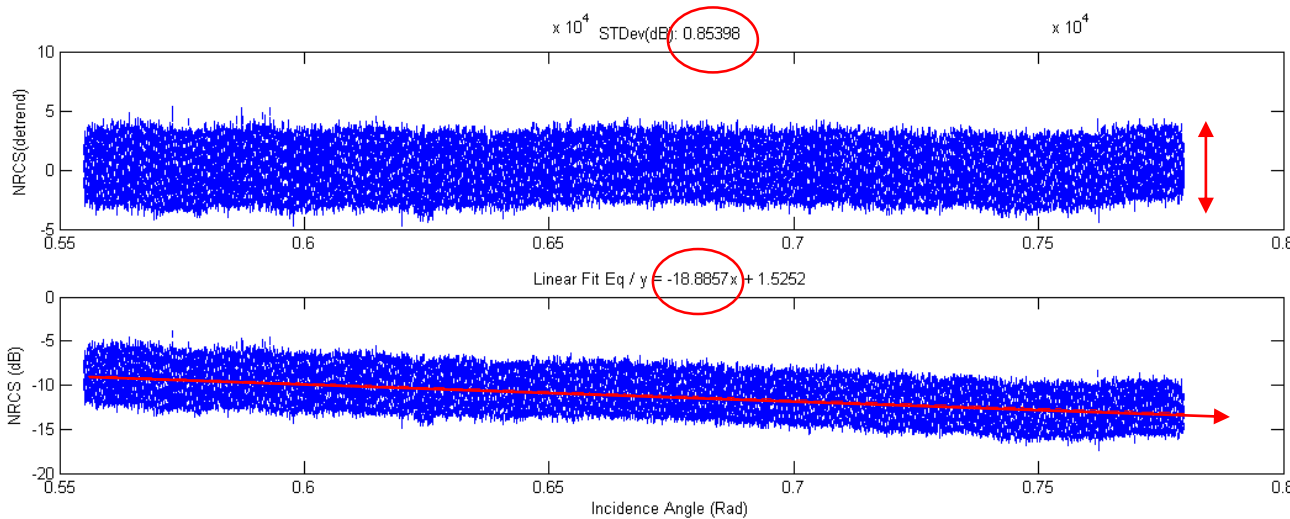


Two subset are taken from each scene:

1. 1000 pixels rectangular subset for empirical standard deviation
2. 1000 pixels width for the entire length of the image for consistent ocean surface slope

Result from 69 scenes plot below :

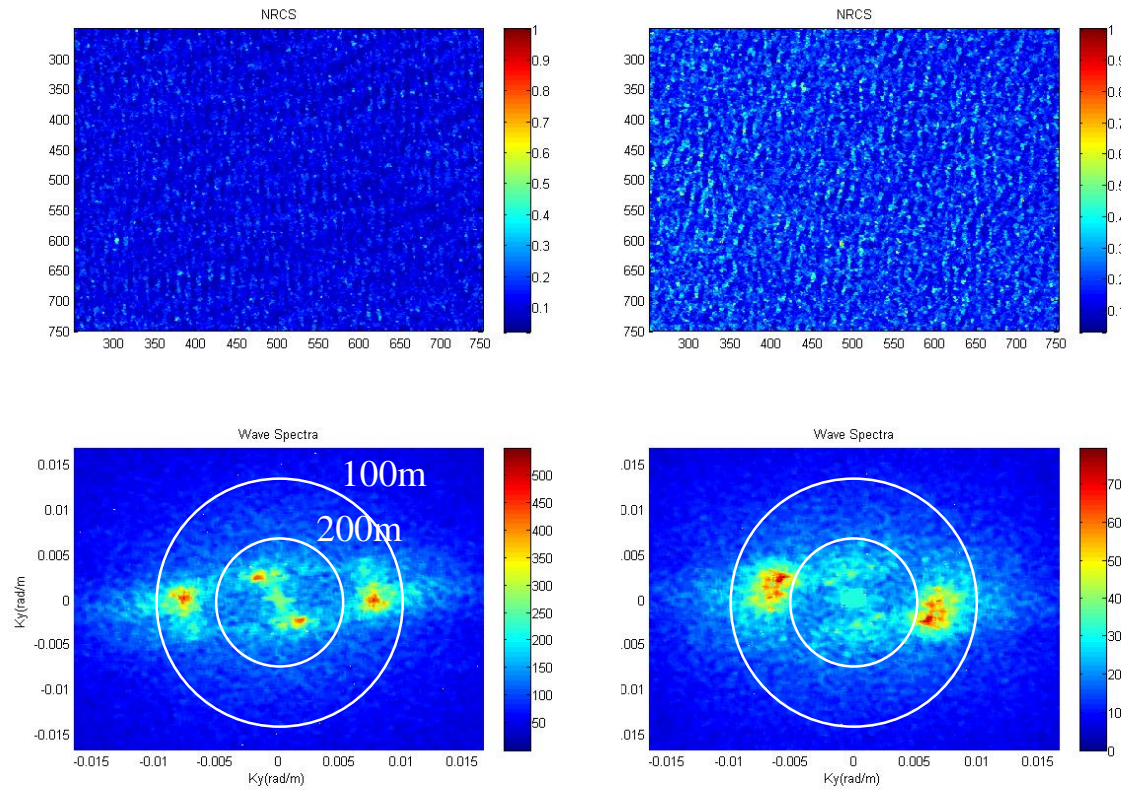
1. The standard deviation (dB) grows stronger with $\gg H_s$
2. The slope (dB/ radians) is relatively steeper with $\gg H_s$



Result

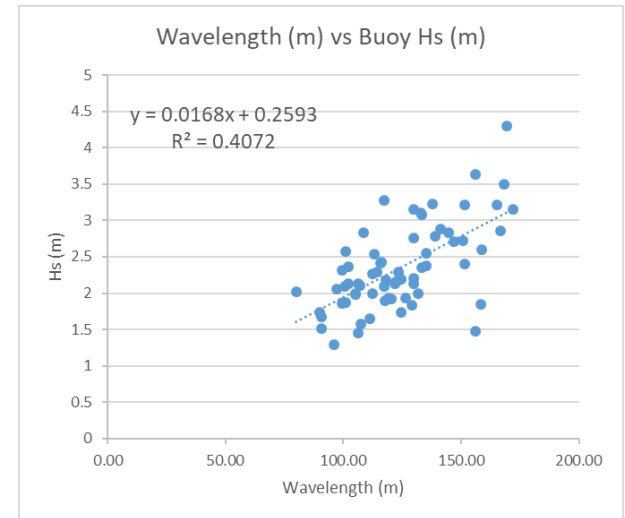
2-Dimensional Fast Fourier Transform (2-D FFT) Wave Spectra Analysis

5x5 pixels parameterized median filter is applied to the radar cross section based on it's effectivity to enhanced the dominant wavelength peak, while 2D Gaussian filter is applied on the frequency domain to reduces the low frequency noise in the middle of the wave spectra.



Dominant WL: 121 m

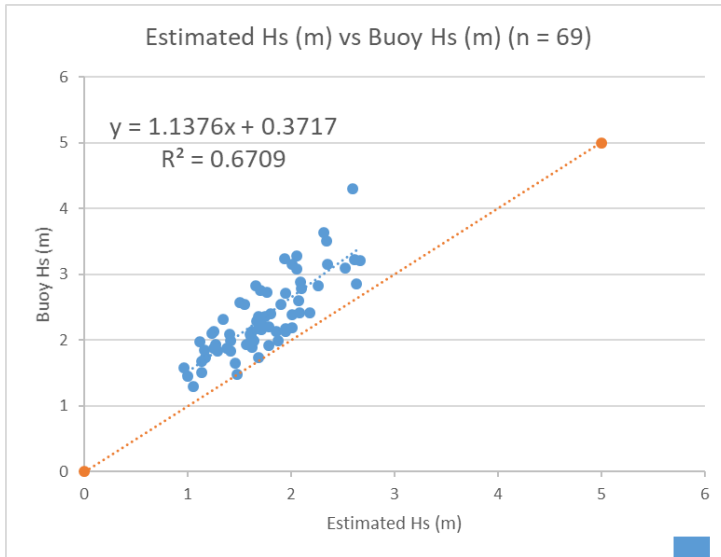
Dominant WL: 158 m



Result from 69 scenes plot below :
The wavelength (m) grows stronger with higher Hs.

Some of the result fails this common pattern due to the high wind speed ($> 10 \text{ ms}^{-1}$) or wind wave dominant sea.

Estimated Hs Result



We found 0.3717m overestimation compared to the buoy data and applied the linear regression

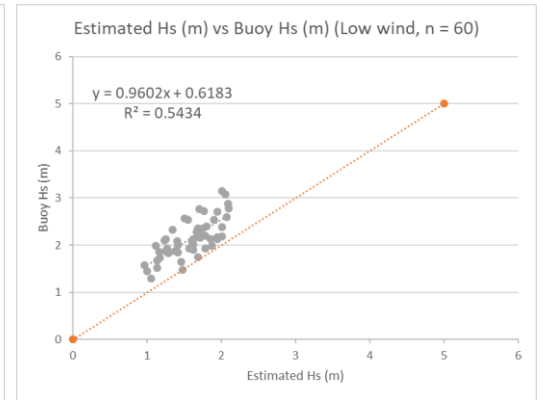
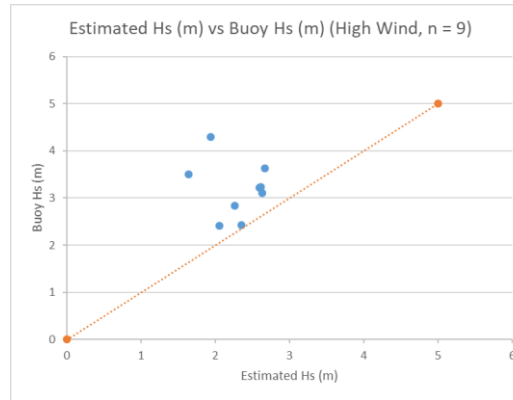
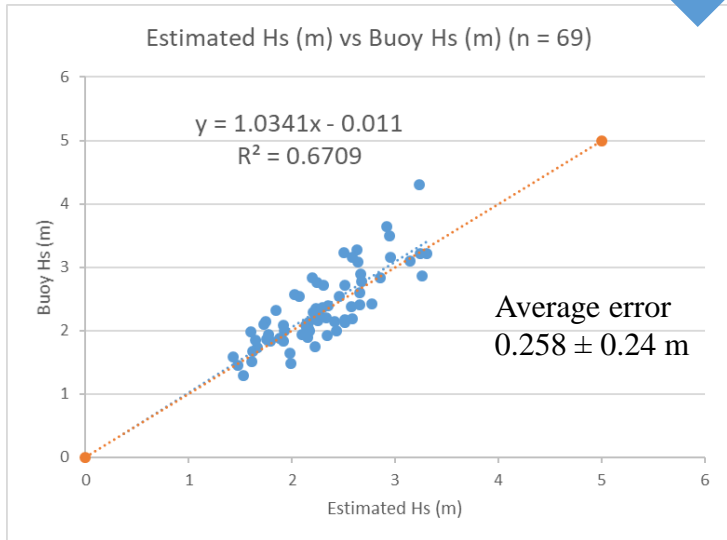


Figure above shows the different between high 10m above sea level wind ($>10\text{ms}^{-1}$) condition (*left*) with low to medium wind speed (*right*) before the linear regression applied

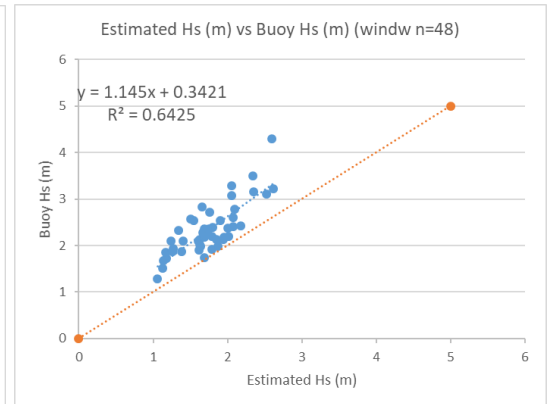
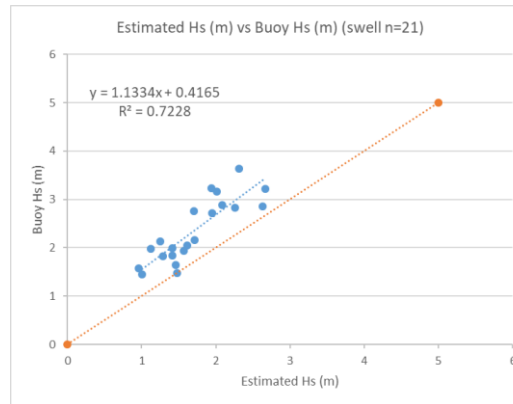
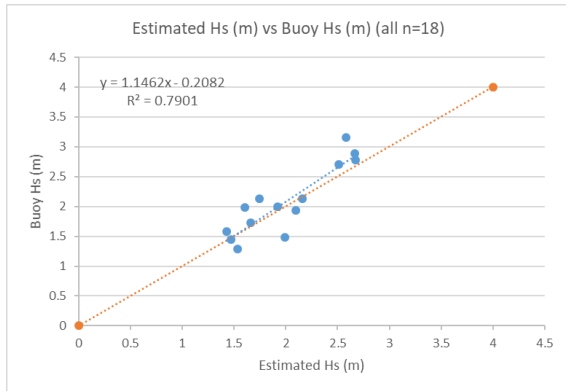


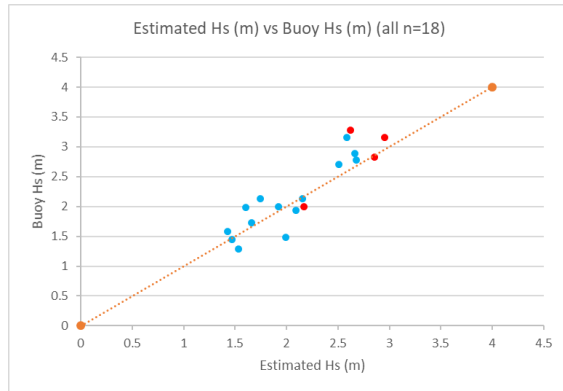
Figure above shows the different between swell dominant sea (*left*), and wind dominant sea (*right*) before the linear regression applied

Estimated Hs Result NBDC51000

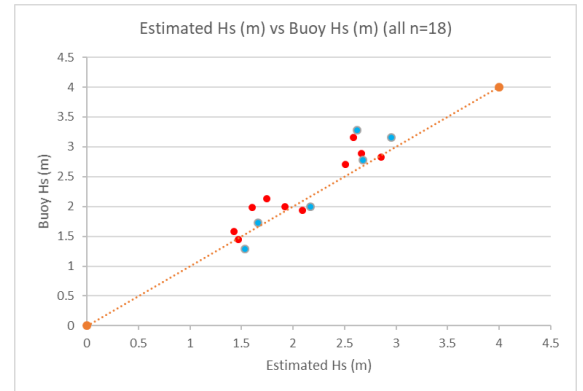
51000 BUOY	STD	SLOPE	WVDIR	WLGTH	Hs	Corr. Hs	WDIR	WSPD	BUOY HS	MWD	Δ Hs		
20161022T042324	0.82564	16.86361	87.51045	144.92754	2.258609	2.85446949	69	10.25	2.83	196.5	0.024469		
20161127T042324	0.853307	12.54231	92.96094	172.41379	2.349041	2.95394481	85.5	11.45	3.155	95.5	0.201055		
20161221T042323	0.914858	10.70636	98.93059	142.85714	2.086743	2.6654168	86.5	8.2	2.885	336	0.219583		
20170303T042320	1.017392	18.58472	93.36646	117.64706	2.050044	2.6250486	110	12.4	3.28	88.5	0.654951		
20170514T042323	0.8224	17.35266	91.59114	138.88889	2.095244	2.67476837	97.5	5.9	2.78	121.5	0.105232		
20170713T042326	0.766734	27.2433	88.76802	107.52688	0.963279	1.42960658	53.5	5.05	1.58	355	0.150393		
20170725T042327	0.930302	27.80714	87.58897	105.26316	1.120971	1.60306778	95.5	6.35	1.98	146	0.376932		
20171005T042330	0.806426	20.94887	92.33731	102.04082	1.250339	1.74537295	66.5	6.55	2.135	124	0.389627		
20171017T042330	0.82886	15.52268	90.84252	147.05882	1.946192	2.51081134	90	3.8	2.71	315.5	0.199189		
20171216T042329	0.970432	35.61468	92.97373	129.87013	2.012276	2.58350401	20	3.6	3.155	319.5	0.571496		
20170426T042240	0.814942	13.01557	98.22672	120.48193	1.567695	2.09446451	75.5	6.3	1.935	184.5	0.159465		
20170520T042241	0.796409	26.8995	89.39049	106.38298	1.002569	1.4728262	107	7.35	1.45	37.5	0.022826		
20170601T042242	0.761406	23.51906	73.951	136.9863	1.411639	1.92280276	80.5	8.2	1.995	308	0.072197		
20170613T042243	0.809963	16.56542	88.19126	105.26316	1.638285	2.17211305	84.5	10.2	1.99	63	0.182113		
20170707T042244	0.765188	22.37789	82.25966	97.087379	1.056724	1.53239669	71	5.1	1.29	69.5	0.242397		
20170719T042245	0.757085	32.67595	67.81599	97.087379	1.173601	1.6609616	86.5	5.5	1.73	48.5	0.069038	MAX	0.654951
20170731T042245	0.791729	26.70793	86.42367	156.25	1.474371	1.99180764	55	5.65	1.48	132	0.511808	STD	0.192493
20170824T042247	0.826893	17.23459	88.17203	106.38298	1.624691	2.15715999	80	8.65	2.125	76.5	0.03216	MEAN	0.232496



All Data



Red : High Wind
Blue: Low- Med Wind



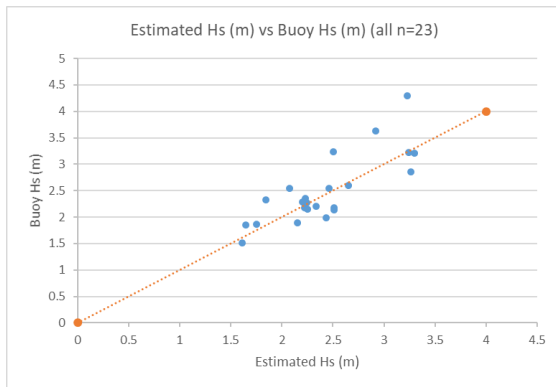
Red : Swell
Blue: Wind Wave

Estimated Hs Result NBDC51004

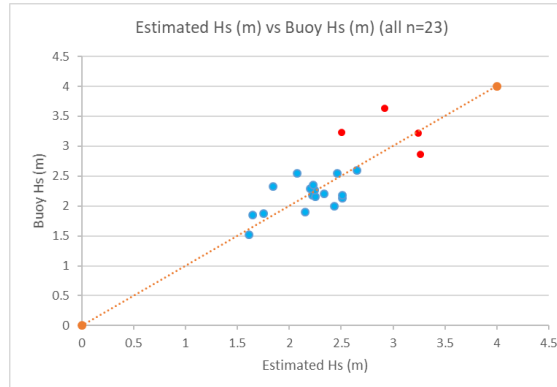
51004 BUOY	STD	SLOPE		WVDIR	WLGTH	Hs	Corr. Hs		WDIR	WSPD	BUOY HS	MWD		Δ Hs
20161022T042140	0.874279	17.63204		91.90915	166.66667	2.630549	3.26360425		53.5	10.9	2.86	215.5		0.403604
20161103T042140	0.865824	26.6801		90.77422	135.13514	1.90089	2.46097924		61	8.2	2.545	84		0.084021
20161115T042140	0.860342	18.16416		97.12502	138.88889	1.941323	2.50545486		68.5	10.9	3.23	300.5		0.724545
20161127T042140	0.911781	12.02273		90.89517	156.25	2.314567	2.91602372		69	12.05	3.635	202		0.718976
20161221T042139	0.935029	17.27665		92.60256	151.51515	2.610188	3.24120675		56.5	10.25	3.22	92.5		0.021207
20170102T042137	0.859727	30.92877		101.5752	120.48193	1.682834	2.22111783		24	3.9	2.18	41		0.041118
20170114T042137	0.852763	11.95477		97.7336	123.45679	1.710419	2.25146141		86	9	2.155	219.5		0.096461
20170303T042136	0.824191	17.52745		90.07441	129.87013	1.943875	2.50826296		106	6.25	2.13	77		0.378263
20170327T042137	0.927765	18.466		97.59464	166.66667	2.665409	3.3019504		77	10	3.215	198		0.08695
20170514T042139	0.803137	16.84089		91.28733	112.35955	1.705629	2.24619159		72.5	8.65	2.27	49.5		0.023808
20170725T042143	0.772183	14.72319		91.28733	112.35955	1.875766	2.43334268		72.5	8.4	1.99	77.5		0.443343
20170806T042144	0.831062	21.88593		92.82712	123.45679	1.666892	2.2035817		61.5	9.55	2.285	87.5		0.081418
20170911T042145	0.772803	25.08942		94.00417	100	1.255533	1.75108595		64	6.9	1.87	101		0.118914
20170426T042056	0.84585	24.70967		90.74406	129.87013	1.784686	2.33315444		79	7.95	2.2	97.5		0.133154
20170508T042056	0.797363	16.08628		87.17288	123.45679	1.947896	2.5126858		101.5	8.35	2.175	57		0.337686
20170520T042057	0.800546	18.52198		89.32596	117.64706	1.618566	2.15042231		64.5	7.45	1.895	85.5		0.255422
20170601T042058	0.805121	15.24979		88.1817	158.73016	2.076251	2.65387633		66	9.75	2.6	107.5		0.053876
20170719T042101	0.765665	24.98263		90.52086	90.909091	1.13085	1.61393496		78	6.25	1.515	118		0.098935
20170812T042102	0.771141	21.10514		95.14276	100	1.163042	1.64934631		64	8.35	1.855	82		0.205654
20170824T042102	0.796415	18.94568		95.14276	100	1.338071	1.84187827		60.5	9.05	2.32	92.5		0.478122
20171023T042104	0.805779	18.83365		95.19443	113.63636	1.547565	2.07232189		82	7.15	2.54	101.5		0.467678
20171116T042104	0.779714	25.38383		90.7639	133.33333	1.689015	2.22791613		46	8.7	2.355	30.5		0.127084
20171128T042104	0.944	17.29433		90.97102	169.49153	2.599436	3.22937918		69	11.25	4.3	18		1.070621

NDBC 51004

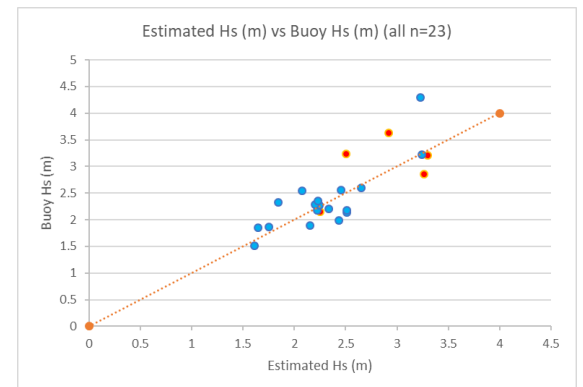
MAX	1.070621
STD	0.273382
MEAN	0.280472



All Data



Red : High Wind
Blue: Low- Med Wind



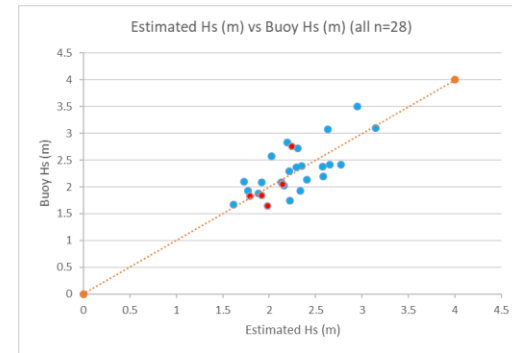
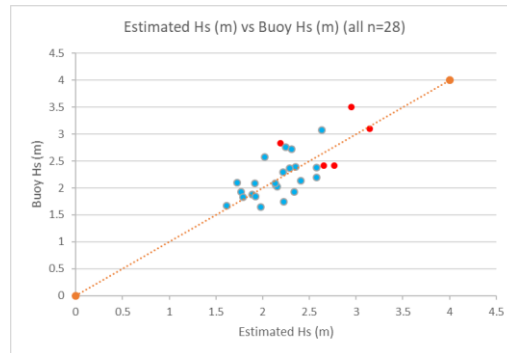
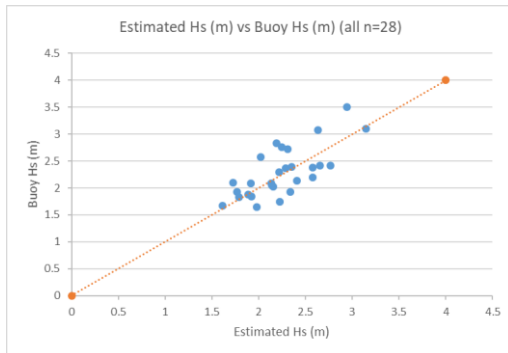
Red : Swell
Blue: Wind Wave

Estimated Hs Result NBDC51002

51002 BUOY	STD	SLOPE	WVDIR	WLGTH	Hs	Corr. Hs	WDIR	WSPD	BUOY HS	MWD	Δ Hs
20161101T043802	0.93716	15.76064	95.33216	133.33333	2.523646	3.14601088	63.5	10.9	3.1	76	0.046011
20161207T043801	0.957645	20.53878	91.54816	135.13514	2.005619	2.57618106	62	4.25	2.38	73	0.196181
20161231T043800	0.90657	17.39849	90.55625	97.087379	1.610286	2.14131414	55.5	6.7	2.05	353	0.091314
20170124T043758	0.962109	22.16477	96.76617	169.49153	2.341849	2.94603405	61	9.95	3.5	83	0.553966
20170301T043758	0.848465	40.2201	85.95551	101.0101	1.406476	1.91712355	104	9.35	2.09	92	0.172876
20170313T043758	0.910571	15.47803	67.16635	86.802224	1.62547	2.1580173	78.5	5.45	2.02	106	0.138017
20170406T043759	0.849394	17.78919	90.69869	121.95122	1.853485	2.40883369	61	8.8	2.135	90.5	0.273834
20170418T043759	0.789169	18.64423	94.28915	125	1.684169	2.22258622	63	7.45	1.74	75	0.482586
20170512T043800	0.830928	13.55441	90.57873	101.0101	1.377407	1.88514715	80.5	8.1	1.875	68	0.010147
20170524T043801	0.853679	18.25362	92.89127	101.0101	1.503698	2.02406753	70	8.5	2.57	63.5	0.545932
20170605T043802	0.864833	18.55678	92.75911	120.48193	1.787317	2.33604877	45.5	8.15	1.925	88	0.411049
20170629T043803	0.890337	7.050044	95.90614	114.94253	1.679457	2.21740304	75	8.15	2.295	81	0.077597
20170711T043804	0.773549	19.75932	90.52086	90.909091	1.132853	1.61613832	59.5	6.65	1.675	79.5	0.058862
20170723T043804	0.901249	24.13868	92.60256	151.51515	1.800684	2.35075191	75	5.7	2.395	82.5	0.044248
20170816T043806	0.829031	22.96289	96.07634	107.52688	1.235696	1.72926515	79	7.65	2.1	95	0.370735
20170921T043807	0.913726	18.10003	95.71059	125	2.008616	2.57947787	60	8.1	2.19	71	0.389478
20171015T043808	0.829466	14.45828	94.03771	117.64706	1.60145	2.13159496	68	8.5	2.09	79	0.041595
20171202T043807	0.899607	21.83215	90.74406	129.87013	1.703396	2.24373528	65	8.8	2.76	350	0.516265
20171226T043806	0.8544	27.07289	93.62148	126.58228	1.271597	1.76875719	102	7.2	1.93	61	0.161243
20170424T043717	0.855724	15.24808	93.99091	116.27907	2.077163	2.65487881	72	10	2.41	98	0.244879
20170506T043718	0.842172	15.65585	92.33731	102.04082	1.747222	2.29194444	69	8.7	2.36	85	0.068056
20170518T043719	0.895909	24.53152	96.05419	151.51515	1.76135	2.30748478	81	9.4	2.72	80	0.412515
20170705T043721	0.8964	15.20925	91.33222	116.27907	2.181453	2.76959846	65	10	2.42	84	0.349598
20170729T043723	0.85764	30.73492	92.72631	158.73016	1.409881	1.92086858	39	9	1.84	88	0.080869
20170810T043723	0.784609	14.10786	101.5601	113.63636	1.463203	1.97952327	73	8	1.65	124	0.329523
20170903T043724	0.842839	27.0111	96.66666	129.87013	1.289917	1.78890862	58	5.4	1.83	173	0.041091
20171021T043726	0.940383	7.975539	90.7639	133.33333	2.057678	2.63344608	61	8.7	3.08	66	0.446554
20171126T043725	0.904022	18.88573	91.86768	108.69565	1.656179	2.1917973	63	10.9	2.83	60	0.638203

NDBC 51002

MAX	0.638203
STD	0.193136
MEAN	0.256901



All Data

Red : High Wind
Blue: Low- Med Wind

Red : Swell
Blue: Wind Wave



Research Objective

1. Evaluating semi-empirical update of significant wave height (H_s) estimation applied to Sentinel-1 SAR repository for narrow-band swell-wave spectrum on the open-ocean waters **without prior knowledge or external inputs**.
2. Evaluate the dependency between H_s and local environment (wind forcing, wave type, SAR system limitation, and imaging mechanism)

Answering our objective, our preliminary findings are as follow :

1. The surface roughness and slope variation parameters update shown consistent result
The wavelength (m) grows longer, standard deviation (dB) grows bigger, and The slope (dB/ radians) is relatively steeper with increasing H_s . Some of the result fails this common pattern due to the high wind speed ($> 10 \text{ ms}^{-1}$) or wind wave dominant sea.
2. Results show that the proposed method performs well in estimating H_s in the low to moderate wind forcing conditions (4 - 10 ms^{-1}) under any wave type in open-water areas. Lower performances are shown in strong wind conditions, and wind wave dominant environment.
3. Two dimensional median filter (with 5×5 pixels kernel size) in spatial domain and two dimensional Gaussian filter (0.0001 wavenumber/ 1km wavelength) in frequency domain are sufficient to remove outlier or noise which resulting more consistent result between varying scenes